Featured Article

Hypoxia and Photofrin Uptake in the Intraperitoneal Carcinomatosis and Sarcomatosis of Photodynamic Therapy Patients

Theresa M. Busch,[1] Stephen M. Hahn,[1,6] E. Paul Wileyto,[2] Cameron J. Koch,[1] Douglas L. Fraker,[3] Paul Zhang,[4] Mary Putt,[5] Kristen Gleason,[1] Daniel B. Shin,[1] Michael J. Emanuele,[1] Kevin Jenkins,[1] Eli Glatstein,[1] and Sydney M. Evans[1]

Departments of [1]Radiation Oncology, [2]Psychiatry, [3]Surgery, [4]Pathology, [5]Biostatistics and Epidemiology, and [6]Division of Hematology-Oncology, University of Pennsylvania, Philadelphia, Pennsylvania

ABSTRACT

Purpose: **Response to photodynamic therapy depends on adequate tumor oxygenation as well as sufficient accumulation of photosensitizer in the tumor. The goal of this study was to investigate the presence of hypoxia and retention of the photosensitizer Photofrin in the tumors of patients with intra-abdominal carcinomatosis or sarcomatosis.**

Experimental Design: **Tumor nodules from 10 patients were studied. In nine of these patients, hypoxia was identified in histological sections of biopsied tumor after administration of the hypoxia marker 2-(2-nitroimidazol-1[*H*]-yl)-*N*-(2,2,3,3,3-pentafluoropropyl)acetamide (EF5). In separate tumor nodules from 10 patients, Photofrin uptake was measured by fluorescence after tissue solubilization.**

Results: **Hypoxia existed in the tumors of five patients, with three of these patients demonstrating at least one severely hypoxic nodule. Physiological levels of oxygen were present in the tumors of four patients. An association between tumor size and hypoxia was not evident because some tumor nodules as small as ~2 mm in diameter were severely hypoxic. However, even these tumor nodules contained vascular networks. Three patients with severely hypoxic tumor nodules exhibited moderate levels of Photofrin uptake of 3.9 ± 0.4 to 3.9 ± 0.5 ng/mg (mean ± SE). The four patients with tumors of physiological oxygenation did not consistently exhibit high tumor concentrations of Photofrin: mean ± SE drug uptake among these patients ranged from 0.6 ± 0.8 to 5.8 ± 0.5 ng/mg.**

Conclusions: **Carcinomatosis or sarcomatosis of the i.p. cavity may exhibit severe tumor hypoxia. Photofrin accumulation in tumors varied by a factor of ~10× among all patients, and, on average, those with severe hypoxia in at least one nodule did not demonstrate poor Photofrin uptake in separate tumor samples. These data emphasize the need for reconsideration of the generally accepted paradigm of small tumor size, good oxygenation, and good drug delivery because this may vary on an individual tumor basis.**

INTRODUCTION

Carcinomatosis or sarcomatosis of the peritoneal cavity is characterized by the presence of tumor nodules on serosal surfaces throughout the abdomen. Tumors that may spread in this pattern include gynecological and gastrointestinal malignancies (1) and sarcomas such as gastrointestinal stromal tumors [GISTs (2)]. Overall, the prognosis is poor for such patients, and surgery alone is generally ineffective in their treatment. Several multimodal therapies are under investigation, including intraoperative or postoperative i.p. chemotherapy (3), hyperthermic i.p. intraoperative chemotherapy (4), and intraoperative i.p. photodynamic therapy [PDT (5)].

PDT may be well suited for the treatment of superficial or microscopic disease remaining after surgical debulking. Feasibility of this approach was demonstrated in a Phase I study of intraoperative Photofrin PDT after debulking surgery of i.p. disease (6), and a Phase II trial has recently been completed (5). The efficacy of this modality is determined by the simultaneous presence of the required components for PDT: photosensitizer; oxygen; and light. However, little to no investigation of these crucial parameters has been conducted for patients with i.p. disease. The presence of pretreatment hypoxia in these nodules is of concern for several reasons. First, hypoxia itself has been found to be a useful prognostic factor for predicting poor outcome to cancer treatment (7), especially radiotherapy (8–10). Although a similar clinical study has not been conducted for PDT, it is likely to be important, given the oxygen dependence of currently used PDT agents, as shown in preclinical studies (11, 12). Secondly, hypoxia can develop or become more severe during illumination due to photochemical oxygen consumption and the vasoconstrictive effects of PDT (11, 13). In one study on patients with basal cell carcinomas undergoing PDT, significant treatment-induced hypoxia has been documented (14). Finally, the presence of hypoxia may indicate an insufficient vascular network that could limit photosensitizer delivery.

The presence of hypoxia in i.p. nodules can be determined by labeling with a hypoxia marker such as the 2-(2-nitroimidazol-1[*H*]-yl)-*N*-(2,2,3,3,3-pentafluoropropyl)acetamide (EF5). In preclinical studies, tumor hypoxia as labeled by EF5 directly

Received 2/24/04; revised 4/22/04; accepted 4/28/04.
Grant support: National Cancer Institute Grants CA75285, CA85831, and CA87971. Partial support for patient care was from USPHS Research Grant M01-RR0040.
The costs of publication of this article were defrayed in part by the payment of page charges. This article must therefore be hereby marked *advertisement* in accordance with 18 U.S.C. Section 1734 solely to indicate this fact.
Requests for reprints: Theresa M. Busch, Department of Radiation Oncology, B13 Anatomy Chemistry Building, 3620 Hamilton Walk, Philadelphia, PA 19104-6072. Fax: (215) 898-0090; E-mail: buschtm@mail.med.upenn.edu.

correlates with radiation resistance (15). A Phase I trial of EF5 has been completed to detect hypoxia in tumors from patients, including those with sarcomas (16), squamous cell carcinomas (17), and other tumor types (18). Data from Phase II trials suggest that hypoxia, as measured by EF5 binding, correlates to other clinically relevant end points, such as tumor necrosis and cytokine regulation (18–20).

The purpose of the present study is to quantify levels of hypoxia and Photofrin in i.p. tumor nodules of patients entered into a Phase II i.p. PDT trial. Data on EF5 binding and Photofrin uptake are reported for multiple tumor nodules per patient in cases where >1 sample could be obtained; however, hypoxia and photosensitizer content were evaluated in separate tumor nodules from each patient. Our data show that a range in EF5 binding and Photofrin uptake is present in tumor specimens. Severe hypoxia could be detected in even the smallest nodules (~2 mm) evaluated. In patients with severely hypoxic tumor nodules, moderate levels of tumor Photofrin uptake were found, whereas low Photofrin uptake was found in the tumors of some patients with nodules of physiological oxygenation.

MATERIALS AND METHODS

Human Subjects. Tissues from 10 patients were studied for Photofrin uptake; 9 of these patients were also studied for tumor hypoxia. Patients were either enrolled separately on the Phase I EF5 trial and the Phase II i.p. PDT trial or enrolled on a trial of EF5 specifically designed for patients undergoing i.p. PDT (alternately, some patients were treated off-study as a compassionate exception to the i.p. PDT trial). The Phase I trial of EF5 was initiated in February 1998, and the EF5 trial for patients undergoing i.p. PDT was initiated in October 2002. The Phase II trial of PDT for disseminated i.p. malignancies began in April 1997. All trials were approved by the Institutional Review Board of the University of Pennsylvania and the Clinical Trials Scientific Review and Monitoring Committee of the University of Pennsylvania. The i.p. PDT trial was approved under an investigator-sponsored IND with the United States Food and Drug Administration. The EF5 trials were approved by Cancer Therapy Evaluation Program, National Cancer Institute. Exclusion and inclusion criteria for these trials have been published previously (5, 16). Patients provided separate written informed consent for each trial. For the patients enrolled separately on the Phase I EF5 and Phase II i.p. PDT trials, EF5 biopsy was performed at a laparoscopy for staging and assessment for treatment with i.p. PDT. Therefore, the time between EF5 biopsy and Photofrin injection was 3 weeks (patient 5), 8 weeks (patient 2), and 14 weeks (patient 1). In all other patients, who were enrolled on the joint EF5 and i.p. PDT trial, EF5 and Photofrin were administered on the same day: biopsy and PDT treatment took place 48 h later. Biopsies for EF5 and Photofrin analysis were collected before illumination was begun.

Drugs Administered. EF5 was supplied by Cancer Therapy Evaluation Program, National Cancer Institute, in vials containing 300 mg of drug plus 100 ml of water with 5% dextrose and 2.4% alcohol. EF5 solution was administered via a peripheral i.v. catheter at a rate no greater than 350 ml/h. Total infusion time was 1–1.5 h, depending on the total dose (12 or 21 mg/kg) administered. Tissue biopsy for EF5 binding was performed 24–48 h later. Binding was corrected for dose and time of drug exposure as described below.

Photofrin was supplied by Axcan Pharma Inc. (Mont-Saint-Hilaire, Quebec, Canada) and administered i.v. at 2.5 mg/kg. Surgical debulking and intraoperative PDT were performed 48 h later. Full treatment details on the i.p. PDT trial have been published previously (5).

Immunohistochemistry. Individual tumor nodules were excised (intact, if possible), put in iced EXCELL 610 media (JRH Biosciences, Leneka, KS) with 15% FCS, transported to the laboratory, and frozen in Tissue Tek OCT (Sakura Finetek USA, Inc., Torrence, CA). Cryosectioning and immunohistochemistry were performed as described previously (21). Briefly, 10-μm sections were fixed in 4% paraformaldehyde, blocked, and stained with EF5 monoclonal antibody (ELK3-51) conjugated to Cy3 dye ("regular stain"). Multiple slide series were cut from some nodules, in which each series was from a different level of the nodule. Sectioning levels were separated by at least 0.5 mm, with each successive level cut at greater distances from the tumor periphery. In addition to the regularly stained sections, within each slide series two sections were stained without antibody to assess endogenous tissue fluorescence ("no stain"). To assess nonspecific antibody binding, sections were stained with an antibody solution containing 0.5 mM EF5, whereby the free EF5 in the solution competed with tissue-bound EF5 for available antibody ("competed staining").

Some tissue sections were additionally stained for CD31 to determine tumor vascularization. Slides to be exposed to CD31 antibody were blocked overnight in PBS containing 1.5% albumin and 0.3% Tween 20 ("antibody carrier") supplemented with 5% skim milk and 5% rat serum. Staining (1.5 h at room temperature) in primary antibody was carried out with mouse antihuman CD31 (PharMingen, San Diego, CA) diluted 1:100 in antibody carrier. After rinses in PBS with 0.3% Tween 20, secondary antibody staining (1:100 in antibody carrier) was carried out at room temperature for 45 min with Cy5-conjugated rat antimouse IgG (Jackson ImmunoResearch, West Grove, PA). Sections were rinsed in PBS with 0.3% Tween 20, followed by fixation of CD31 labeling for 20 min in 4% paraformaldehyde. Staining for EF5 was then performed as described above.

Fluorescence Photography. Fluorescence microscopy (LabPhot microscope with a 100-W high-pressure mercury arc lamp and Photometrics Quantix charge-coupled device digital camera) was carried out as described previously (17). An automatic stage (Ludl Electronic Products) and IP Lab Spectrum software (Scanalytics, Fairfax, VA) precisely controlled stage movement for the purpose of photography of the entire section. Immediately before photography, slides were flooded with a solution of Hoechst 33342 (20 μM in PBS) to label the DNA of individual cells in the photographed images. Photographs were taken using filter cubes appropriate for Cy3 [EF5 or 2-(2-nitroimidazol-1 [*H*]-yl)-*N*-(3,3,3-trifluoropropyl)acetamide (EF3)], Cy5 (CD31), and Hoechst 33342. At the beginning and conclusion of each camera session, an image of hemacytometer-loaded calibration dye (a standard concentration of Cy3 in 1% paraformaldehyde) was taken. The fluorescence of this dye was defined as "1000." The fluorescence of other images was then

determined by comparing their brightness with the calibration dye, with correction for camera shutter exposure.

Analysis of *in situ* EF5 Binding. For the purpose of image analysis, bitmap (two-color) masks were created of the Hoechst 33342 images in Adobe PhotoShop (Adobe Systems, Inc., San Jose, CA) by applying the auto level function to enhance contrast followed by maximize and median filters to spread the nuclear-localized fluorescence over the approximate diameter of a cell. Thresholding was performed to create a mask of tissue-containing areas. Images were analyzed using routines written in MatLab (The MathWorks, Inc., Natick, MA), whereby EF5-dependent fluorescence intensity values were sampled within an image based on tissue location identified by the Hoechst 33342 mask. Because of limitations in memory, images analyzed in MatLab were cropped to a maximum of 1200 × 1200 pixels for analysis.

EF5 intensity values at the 95% binding level were determined from EF5 binding in all tumor tissue on a section, identified by the Hoechst mask. The 95% binding values were calibrated based on lamp intensity and exposure time (see "Fluorescence Photography") and normalized for total EF5 drug exposure in individual patients. Total drug exposure was calculated (in μM·h) based on the area under the curve plotted from drug concentration at the time of EF5 infusion and at the time of tissue biopsy (22). Final values for *in situ* EF5 binding were obtained by subtracting the value for nonspecific binding (competed stain) in an adjacent section from that of regular stain binding.

Determination of Cube Reference Binding. Cube reference binding was used to determine the maximum possible EF5 binding in tumor tissue from each patient. This was performed as described previously (17). Briefly, tissue cubes were dissected from the fresh biopsy and incubated *in vitro* in the hypoxia marker EF3 (200 μM for 3 h) under low oxygen concentration (0.2%). Hypoxia marker binding values in the reference cubes were multiplied by the ratio of total drug exposure in the reference (600 μM·h) to that in the patient (based on area under the curve). The drug EF3 (similar to EF5, but containing three fluorines instead of five) was used for these studies to minimize any contribution from EF5 binding that had occurred *in situ* (*i.e.,* antibodies against EF3 do not bind strongly to EF5). Respiration created maximum EF3 binding at several cell layers beneath the surface of the cube. Sections cut from these layers were stained for EF3 binding using an EF3-specific monoclonal antibody (ELK5-A8). In photographed images, the median EF3-dependent fluorescence intensity in areas of maximum binding was determined using Adobe PhotoShop. The magic wand function was used to highlight regions ≥20 (range, 0–255) fluorescence intensity units higher than background. For each specimen/level, the percentage of cube reference binding was determined by dividing the *in situ* binding at the 95% level by the median cube reference binding determined from a specimen cube from the same patient.

Analysis of Photofrin Uptake. In general, the small mass of the tumor nodules collected for the EF5 study prohibited the evaluation of hypoxia and Photofrin uptake in the same tumor sample, but up to an additional seven tumor nodules were collected from each patient for Photofrin assay. Whole tumor nodules or biopsies of larger disease were resected in the operating room, placed in specimen containers, protected from visible light, and frozen at −80°C. Whenever possible, sizes of the tumor nodules collected for Photofrin uptake were similar to those studied for EF5 binding. The spectrofluorometric assay for Photofrin quantification was based on a previous report (23). Tissue samples were thawed to room temperature, weighed, and, depending on the amount available, ~10–50 mg of tissue were placed in a vial with 0.150–0.500 ml of the tissue solubilizer, Solvable (Packard, Meriden, CT). The vial was capped and heated at 50°C overnight (20 ± 2 h) in the dark. The following day, the solution was cooled to room temperature, mixed with an equal volume of distilled water, and transferred to a quartz cuvette of 200 μl (10-mg samples) or 600 μl (50-mg samples) capacity. The fluorescence of the solubilized sample was measured by a spectrofluorometer (FluoroMax-3; Jobin Yvon, Inc., Edison, NJ) with λ_{ex} of 405 nm and λ_{em} of 627 nm. Photofrin concentration in the tissue was calculated based on the increase in fluorescence resulting from the addition of a known amount of Photofrin to each sample after its initial reading. Data are presented as nanograms of Photofrin per milligram of tissue for each unique sample. If tissue mass was sufficient, samples were run in replicate and averaged.

Statistics. Analyses were carried out using R 1.70. Both simple descriptive statistics (sample medians and ranges) and linear models were used to describe the data. With respect to hypothesis testing, because our sample size was small, we considered each patient to be of interest, rather than trying to group patients by histology or strata and testing for differences between groups. For the EF5 data, likelihood ratio tests were constructed using mixed effects models to determine whether there were statistically significant differences in EF5 binding among patients (24). This model took into account the correlation among tumors within individual patients (interspecimen variability) and the correlation among sections within individual tumors (intraspecimen variability). For the EF5 data, we also modeled the variance both within and between tumors as an increasing function of the mean EF5 uptake per subject. This approach was based on initial exploratory analyses. For the Photofrin data, we carried out a one-way ANOVA to determine whether there were differences between individuals. Statistical tests were two-sided, with statistical significance declared if the P for a test was <0.05.

RESULTS

Patient Information. All patients had carcinomatosis or sarcomatosis of the i.p. cavity. Histological diagnoses included GIST ($n = 2$; patients 1 and 2), ovarian carcinoma ($n = 2$; patients 3 and 4), colon carcinoma ($n = 3$; patients 5–7), small bowel carcinoma ($n = 1$; patient 8), and appendiceal carcinoma ($n = 2$; patients 9 and 10). In patient 10, tumor nodules were analyzed for Photofrin uptake but not for EF5 binding because of difficulties in obtaining the blood samples necessary to determine total EF5 exposure (see "Analysis of *in Situ* EF5 Bind-

Table 1 EF5 binding in intraperitoneal malignancies

Patient no.	Histology	Cohort	Specimen	Sectioning levels	% of reference binding at each level[a]	Intraspecimen median (range)[b]	Interspecimen median (range)[c]	Interspecimen mean (SE)[d]
1	GIST[e]	Sarcoma	A	1, 2, 3, and 4	0.3, 0.1, 0.2, and 0.6	0.3 (0.5)	0.2 (0.3)	0.4 (0.5)
			B	1, 2, and 3	0, 0, and 0.7	0.0 (0.7)		
2	GIST	Sarcoma	A	1, 2, and 3	1.4, 1.4, and 1.1	1.4 (0.3)	1.4	1.4 (1.7)
3	Ovarian CA	Ovarian	A	1 and 2	6.3 and 4.7	5.5 (1.6)	5.5 (6.2)	5.1 (2.8)
			B	1	8.3	8.3		
			C	1 and 2	1.8 and 2.3	2.1 (0.5)		
4	Ovarian CA	Ovarian	A	1	3.2	3.2	3.2 (67.5)	26.2 (11.0)
			B	1 and 2	95.3 and 44.1	69.7 (51.2)		
			C	1 and 2	2.8 and 1.6	2.2 (1.2)		
5	Colon CA	GI	A	1	6.0	6.0	6.2 (32.8)	15.0 (7.5)
			B	1 and 2	22.4 and 54.9	38.7 (32.5)		
			C	1	6.4	6.4		
			D	1	5.9	5.9		
6	Colon CA	GI	A	1	50.0	50.0	29.7 (35.9)	29.2 (10.1)
			B	1	18.4	18.4		
			C	1 and 2	8.5 and 19.7	14.1 (11.2)		
			D	1	40.9	40.9		
7	Colon CA	GI	A	1 and 2	2.3 and 1.6	2.0 (0.7)	8.6 (15.4)	8.3 (3.2)
			B	1 and 2	18.7 and 16.0	17.4 (2.7)		
			C	1 and 2	13.3 and 4.7	9.0 (8.6)		
			D	1 and 2	2.5 and 14.6	8.6 (12.1)		
			E	1 and 2	5.1 and 4.5	4.8 (0.6)		
8	Small bowel CA	GI	A[f]	1, 2, and 3	2.3, 0.2, and 1.3	1.3 (2.1)	1.3	1.4 (1.7)
9	Appendiceal CA	GI	A	1	0.3	0.3	0.3 (1.5)	1.0 (1.3)
			B	1	0.2	0.2		
			C	1 and 2	1.6 and 1.7	1.7 (0.1)		

[a] EF5 binding is expressed as a percentage of maximum hypoxia marker binding in tissue from the same patient. Reference binding values were not available for patients 4, 7, and 9. For these patients, the percentage of reference binding was calculated based on the average reference binding level in other patients of the same disease cohort.

[b] Median and range (largest-smallest) of values for each specimen.

[c] Median and range (largest-smallest) of median values of specimens for each patient.

[d] The model-based mean and SE of specimens for each patient.

[e] GIST, gastrointestinal stromal tumor; CA, carcinoma.

[f] An additional three specimens from patient 8 were found by histological analysis to contain no tumor and are thus not included in these data.

ing" in "Materials and Methods"). Data on tumor EF5 binding have been reported previously for patients 1 and 2 (16).[7]

EF5 Binding in Tumor Nodules of Intraperitoneal Disease. Table 1 lists EF5 binding in the tumor nodules of nine patients. EF5 binding is quantified as a percentage of the cube reference binding, *i.e.*, a percentage of the maximum binding level possible for the tissue under consideration. The relationship between pO_2 and percentage of cube reference binding, based on *in vitro* calibration studies, has been published previously (25). We have defined the following relationships: physiological oxygenation, 10% oxygen $\approx$ 1% of cube reference binding; modest hypoxia, 2.5% oxygen $\approx$ 3% of cube reference binding; moderate hypoxia, 0.5% oxygen $\approx$ 10% of cube reference binding; and severe hypoxia, 0.1% oxygen $\approx$ 30% of cube reference binding. It should be noted that EF5 binding is extremely sensitive at low oxygen tensions and increases rapidly for small changes in pO_2. Thus, severe hypoxia encompasses a large range of EF5 binding values, *i.e.*, 30–100%.

Substantial variability in EF5 binding was evident in some patients, as measured by the range of recorded values both within levels of the same specimen (intraspecimen) and among specimens from the same patient (interspecimen; Table 1). In general, patients with lower levels of median EF5 binding demonstrated similar intraspecimen and interspecimen variability evidenced by the range in binding, whereas patients with higher binding levels generally exhibited greater overall interspecimen ranges in binding as well as higher interspecimen than intraspecimen variability. The increased interspecimen variability is reflected in the estimated SEs of the mean, based on the mixed effects model. Mean differences in EF5 binding among patients varied greatly, ranging from 0.4 to 26.2, but were not statistically significant ($P = 0.541$), likely because of the large interspecimen variability in those with high EF5 binding.

Low to negligible levels of EF5 binding were found in the tumors of patients with GIST (patients 1 and 2) and small bowel (patient 8) and appendiceal (patient 9) cancer (Table 1). Here, little binding variability was found among different tumor nodules from the same patient or between different levels of the same nodule. The EF5 binding level corresponded to physiological oxygenation of these tumors (Fig. 1). We have previ-

[7] In our previous publication of EF5 binding in human sarcomas (16), tumor areas of highest EF5 binding were reported for the section demonstrating the most severe hypoxia in each patient. In the present report, EF5 binding was measured within all of the tumor tissue in a given section and reported separately for each specimen and sectioning level (Table 1).

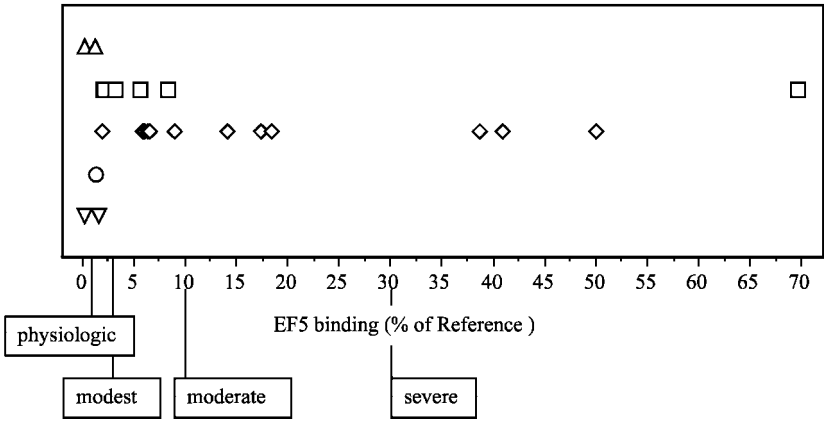

Fig. 1 Hypoxia (EF5 binding) in specimens of i.p. malignancy from patients with gastrointestinal stromal tumor (△), ovarian carcinoma (□), colon carcinoma (◇), small bowel carcinoma (○), or appendiceal carcinoma (▽) who were given the hypoxia marker EF5. EF5 binding is expressed as the average of percentage of reference binding, *i.e.*, maximum hypoxia, over all sectioning levels for a given specimen. EF5 binding levels of 1%, 3%, 10%, and 30% correlate to hypoxia that is physiological, modest, moderate, or severe, respectively.

ously reported (16) low levels of EF5 binding in small nodules of GIST from another patient. The patient was not included in the present study because he was not considered for PDT treatment. However, in this patient, high levels of EF5 binding were found in much larger tumor nodules (1.65 and >6 cm), suggesting that in this tumor type, size may contribute to the development of hypoxic regions. The limited number of GIST samples available precluded any analysis of tumor size *versus* hypoxia within this specific histology.

EF5 binding ≤ 8% of cube reference, corresponding to physiological oxygenation to modest hypoxia, was found in the majority of specimens of ovarian carcinoma from patients 3 and 4 (Table 1, Fig. 1). However, severe hypoxia was found in one of six specimens of ovarian cancer evaluated. Specimen B of patient 4 demonstrated cube reference binding > 30%, *i.e.*, severe hypoxia, at both sectioning levels studied.

In addition to the single specimen of ovarian cancer, specimens of colon carcinoma from all three patients (patients 5–7) demonstrated high levels of EF5 binding (Table 1). Severely hypoxic tumors were detected in patients 4–6, and moderate hypoxia was detected in patient 7. These tumors demonstrated substantial intra- and intertumoral hypoxic heterogeneity compared with GISTs and the small bowel and appendiceal tumors that were well oxygenated. Oxygenation in the colon and ovarian cancers ranged from physiological levels to severely hypoxic (Fig. 1), but in general the intraspecimen variability was smaller than the interspecimen variability (see Table 1). Ovarian cancer (patient 4) demonstrated the broadest interspecimen hypoxic heterogeneity among all nine of the patients studied. However, colon cancer was the most likely histological type to contain moderate to severe hypoxia. Colon cancer, together with small bowel and appendiceal cancer, comprises the gastrointestinal cohort of patients treated on the i.p. PDT trial (5). In the small sample of patients we examined, diseases of different histology within the gastrointestinal cohort demonstrated vastly different levels of hypoxia. These data suggest that it may be worthwhile to stratify future outcome analysis by specific histology, in addition to the more general disease cohort.

Throughout this study, every attempt was made to acquire tumor nodules of ≤5 mm in thickness because PDT is only administered to patients when their disease is debulked to a size of 5 mm or less. However, in some patients, larger tumors were removed and available for analysis. Thus, the size of the nodules sampled was representative of the disease in each patient and varied among individuals. The smallest disease studied was ~1–2-mm nodules of GIST and colon carcinoma. Specimens of ~30- or 45-mm bulky disease were taken of colon and ovarian cancer, respectively. The association between hypoxia and tumor size was evaluated, and no relationship between greatest tumor dimension and EF5 binding was found in tumors from 1 to 45 mm in diameter (Fig. 2). Using a polarographic needle probe (Eppendorf pO_2 Histograph) to measure the oxygenation of tumors (~10 mm diameter or larger) of the breast and the head and neck, others have demonstrated a correlation between decreasing tumor size and decreasing hypoxia in some studies (26), but not in all studies (27, 28). Notably, in the present study, the majority of tumors that we investigated were <10 mm in maximum diameter. Eleven of the 12 sections that demonstrated EF5 binding of ~10% or higher were from tumor nodules of ≤10 mm in greatest dimension. In particular, the single ovarian biopsy that exhibited severe hypoxia was from a nodule 8 mm

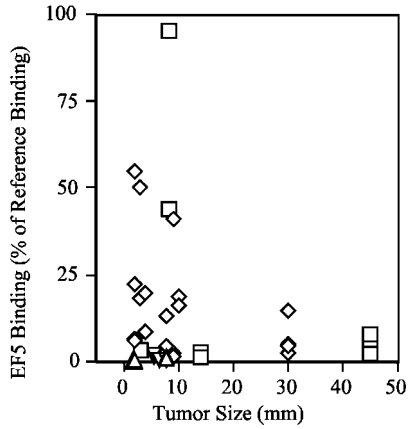

Fig. 2 Hypoxia (EF5 binding) in individual histological sections of i.p. malignancy from patients with gastrointestinal stromal tumor (△), ovarian carcinoma (□), colon carcinoma (◇), or appendiceal carcinoma (▽) *versus* the maximum diameter (in millimeters) of the tumor from which the section was cut. EF5 binding is expressed as a percentage of reference binding, *i.e.*, maximum hypoxia.

in diameter, *versus* the oxic measurements in ovarian specimens measuring 45 mm. The lack of severe hypoxia in larger tumor nodules was not affected by the presence of necrotic tissue, which cannot metabolize EF5, because analysis was conducted only on viable malignant tissue identified by a pathologist on each section. Furthermore, very limited necrosis was detected in the tumors of this study.

EF5 is a vascular-delivered drug; thus, one might hypothesize that avascular tumor nodules could exhibit limited EF5 binding as a consequence of poor drug delivery. We have previously demonstrated (29) the presence of vascular structure in tumor nodules as small as 1–2 mm from patients enrolled on the i.p. PDT trial. To confirm the vascularity of the nodules evaluated for EF5 binding, sections adjacent to those analyzed for EF5 were stained for both EF5 and CD31. Fig. 3 depicts photomicrographs of EF5-identified hypoxia and CD31-labeled vascular structure in representative small tumor nodules (~2 mm) with severe (Fig. 3*A*), modest (Fig. 3*C*), or physiological (Fig. 3*E*) hypoxia. The corresponding tissue areas, identified by Hoechst 33342 staining on each section, are shown in Fig. 3, *B*, *D*, and *F*, respectively. All nodules exhibit well-formed vascular structure, although the size of the vessels may differ between tumors of different histologies (compare colon cancer in Fig. 3, *A* and *C*, with GIST in Fig. 3*E*). CD31 staining does not demonstrate vascular perfusion, but it does indicate the presence of a vascular network in even the millimeter-sized nodules of this study. The adequate delivery of EF5 through this network is evidenced by the presence of EF5 binding in the most vascular-distant cells in micrograph (Fig. 3*A*). Furthermore, in this image, the pattern of increasing hypoxia as a function of distance to the nearest blood vessel (regardless of perfusion) suggests that diffusion-limited hypoxia, as opposed to perfusion-limited hypoxia, predominates. Such a distribution of hypoxia may be relevant to the PDT tumor response (30) because mechanisms of Photofrin PDT damage include insult to malignant cells, which may or may not be located in close proximity to a blood vessel, and damage of the blood vessels themselves.

Photofrin Uptake in Tumor Nodules of Intraperitoneal Disease. Photofrin concentration was measured in tumor nodules that were distinct from those used for EF5, but which were sampled from the same patients studied for EF5 binding. The nodules ranged in size from 1.8 to 20 mm in greatest diameter, and as with the EF5 binding, no association between tumor size and Photofrin uptake was evident (data not shown). The Photofrin uptake in each nodule is listed in Table 2. In contrast to EF5 binding, the variability in Photofrin uptake within patients

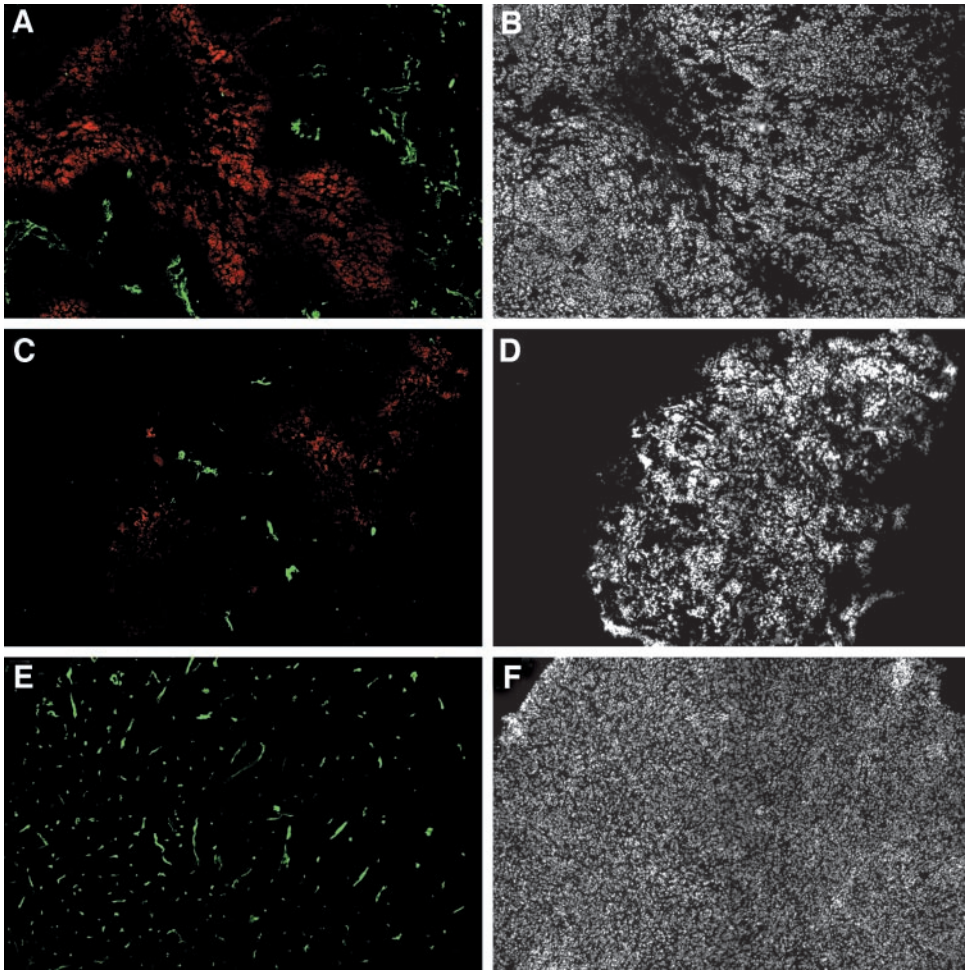

Fig. 3 Images of EF5 binding and CD31 staining (*A*, *C*, and *E*) and Hoechst 33342-labeled tissue (*B*, *D*, and *F*) in ~2-mm specimens of colon carcinoma (*A* and *B*, patient 5, specimen B, level 2; *C* and *D*; patient 5, specimen D, level 1) and gastrointestinal stromal tumor (*E* and *F*, patient 1, specimen B, level 3). EF5 binding is shown in *red*, and CD31 staining is shown in *green*. The level of EF5 binding, *i.e.*, the severity of hypoxia, is indicated by *red color intensity*. Tumors with severe, modest, and physiological hypoxia are depicted in *A*, *C*, and *E*, respectively. Hoechst 33342 was used to label cell nuclei, *i.e.*, tissue-containing areas of the section. The images depict tissue regions of 2.16 × 1.44 mm.

Table 2 Photofrin uptake in intraperitoneal malignancies

Patient no.	Histology	Cohort	Specimen	Photofrin uptake (ng/mg)[a]	Interspecimen median (range)[b]	Interspecimen mean (SE)[c]
1	GIST[d]	Sarcoma	1	1.26	1.26	1.3 (1.1)
2	GIST	Sarcoma	1, 2, and 3	3.28, 1.34, and 0.96	1.34 (2.32)	1.9 (0.6)
3	Ovarian CA	Ovarian	1, 2, and 3	1.99, 3.14, and 2.91	2.91 (1.15)	2.7 (0.6)
4	Ovarian CA	Ovarian	1, 2, 3, and 4	4.44, 5.26, 4.30, and 1.72	4.37 (3.54)	3.9 (0.5)
5	Colon CA	GI	1, 2, and 3 4 and 5	4.63, 2.79, and 4.12 3.32 and 4.49	4.12 (1.84)	3.9 (0.5)
6	Colon CA	GI	1, 2, and 3 4, 5, 6, and 7	3.06, 4.44, and 3.50 4.74, 3.32, 3.84, and 4.36	3.84 (1.68)	3.9 (0.4)
7	Colon CA	GI	1, 2, and 3 4, 5, 6, and 7	0.66, 0.39, and 0.87 0.91, 0.38, 0.77, and 4.27	0.77 (3.89)	1.2 (0.4)
8	Small bowel CA	GI	1, 2, and 3 4 and 5	5.30, 4.79, and 6.40 6.67 and 5.80	5.80 (1.88)	5.8 (0.5)
9	Appendiceal CA	GI	1 and 2	0.98 and 0.13	0.55 (0.85)	0.6 (0.8)
10	Appendiceal CA	GI	1, 2, and 3 4, 5, and 6	0.68, 0.78, and 0.68 3.91, 1.36, and 0.39	0.78 (3.52)	1.3 (0.4)

[a] Drug uptake was measured by fluorescence in whole tumor nodules after tissue solubilization.
[b] Median and range (largest-smallest) of values of specimens for each patient.
[c] The model-based mean (SE) of specimens for each patient.
[d] GIST, gastrointestinal stromal tumor; CA, carcinoma; GI, gastrointestinal.

was reasonably constant and did not vary in any obvious fashion with mean Photofrin level. In patient 7, interspecimen differences in Photofrin uptake were associated with site of biopsy; the first six nodules (uptake range, 0.38–0.91 ng/mg) were excised from the surface of the small bowel, whereas the last nodule (uptake, 4.27 ng/mg) was removed from the surface of the liver. Because normal liver is known to accumulate high levels of Photofrin, it might be expected that tumor nodules from this site would have high Photofrin uptake. Also, some variability in Photofrin uptake among specimens may be accounted for by heterogeneity in endogenous chromophore levels due to sample-to-sample variability in blood volume (23), although the mostly small biopsies of this study were nonhemorrhagic in nature. Overall, differences in Photofrin uptake among individuals were highly significant ($P < 0.0001$).

The highest levels of Photofrin uptake were found in nodules of small bowel cancer resected from the peritoneum of patient 8; average drug uptake was 5.8 ± 0.5 ng/mg. Patients 3 and 4 (ovarian cancer) and patients 5 and 6 (colon cancer) also demonstrated moderate Photofrin uptake with average levels of 2.7 ± 0.6, 3.9 ± 0.5, 3.9 ± 0.5, and 3.9 ± 0.4 ng/mg, respectively. The lowest levels of Photofrin uptake were found in patients 1 and 2 (GIST) and patient 9 (appendiceal cancer), in whom average drug levels were 1.3 ± 1.1, 1.9 ± 0.6, and 0.6 ± 0.8 ng/mg, respectively. These data suggest the presence of disease-dependent trends in Photofrin uptake. We will more rigorously examine the association between disease histology and Photofrin accumulation in a separate, future study that evaluates a larger number of i.p. PDT patients.

In nine patients (patients 1–9) who were evaluated for both Photofrin uptake and EF5 binding, we examined whether patients who had severely hypoxic tumors also demonstrated lower Photofrin uptake in separate nodules of their disease. The presence of diffusion-dependent hypoxia, such as that shown in Fig. 3, could lead to limitations in photosensitizer delivery. Fig. 4 plots the mean concentration of Photofrin in all tumor biopsies from a given patient *versus* the level of hypoxia detected in each patient. Low average Photofrin accumulation was not apparent in patients with severely hypoxic tumors. In fact, among the highest mean Photofrin levels (~4 ng/mg) were detected in the tumor nodules of patients 4–6, who exhibited severely hypoxic tumors (EF5 binding > 30% of cube reference binding). In patients with physiological oxygenation, mean Photofrin uptake ranged from <1 to ~6 ng/mg (Fig. 4), suggesting that low accumulation of Photofrin may be found in minimally hypoxic disease. The low cellularity of some specimens, such as those of appendiceal cancer, may account for some of these findings. Whereas a low tumor cell density minimally affects EF5 analysis, which is based on histologically identified malignancy, low tumor cell density among stroma tissue will affect the Photofrin analysis, which is based on the weight of the excised nodule. As a consequence, among tumor nodules with high stroma content,

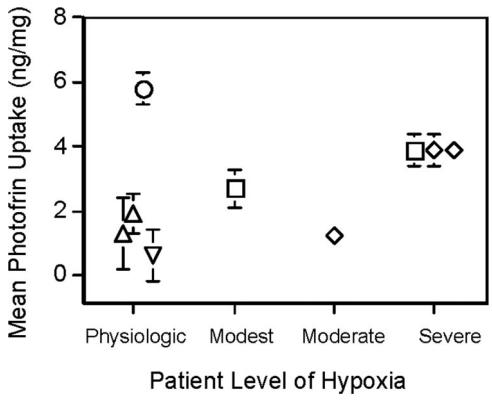

Fig. 4 The mean concentration of Photofrin (nanograms/milligram) *versus* the oxygenation status of the most hypoxic specimen detected in each patient. Photofrin uptake and EF5 binding were measured in separate tumor nodules. *Error bars* are SE. Patients include those with gastrointestinal stromal tumor (△), ovarian carcinoma (□), colon carcinoma (◇), small bowel carcinoma (○), or appendiceal carcinoma (▽).

stromal uptake of Photofrin will contribute greatly to the nodule-averaged photosensitizer level.

DISCUSSION

These data demonstrate substantial inter- and intratumoral hypoxic heterogeneity among different histological tumors that can manifest themselves as carcinomatosis or sarcomatosis. An important conclusion of our investigations is that even a ≤5 mm tumor nodule may be substantially hypoxic because high levels of hypoxia marker binding were found in colon cancer nodules, which were among the smallest nodules evaluated in this study. These data are potentially important to the efficacy of i.p. PDT because PDT is an oxygen-dependent process. Furthermore, because many of the colon cancer nodules demonstrated moderate Photofrin uptake of ~3–5 ng/mg, PDT itself may further contribute to tumor hypoxia through photochemical-induced oxygen depletion. Others have demonstrated that oxygen depletion can occur during PDT of basal cell cancer nodules thought to contain Photofrin in the range of only 0.29–1.59 ng/mg (14).

Vascular networks were present in even the smallest and most severely hypoxic tumors, suggesting a mechanism for tumor uptake of i.v. delivered cancer drugs, such as Photofrin. Vascular networks were also detected in nodules demonstrating low levels of hypoxia, suggesting that EF5 (or Photofrin) delivery was not limited by drug access, although we cannot demonstrate the presence of blood flow in these patient samples. The finding of biopsies that demonstrate low Photofrin uptake in patients who have little EF5 binding in their disease brings to light the possibility that delivery of both agents may have been limited. However, extensive preclinical evaluation has established that under long incubation times, sufficient concentrations of hypoxia marker are delivered to label even low perfusion areas (31–35). Additionally, we always see EF5 binding adjacent to regions of necrosis. In control studies of perfusion-created limitations in hypoxia marker delivery, drug inaccessibility was visible in distinct binding patterns, characterized by high binding areas delineating well-defined "holes" (30). No such binding patterns were found in the clinical samples of the present study, suggesting that EF5 delivery was not a limiting factor.

Technical limitations prevented the examination of Photofrin uptake and EF5 binding in the same tumor nodule. However, in patients with severely hypoxic tumor nodules (patients 4–6), separate tumor specimens demonstrated substantial Photofrin uptake. Based on these data, we suggest that the currently accepted paradigms of the relationships among tumor size, vascular distribution, drug delivery, and hypoxia must be reconsidered because they may be much too general. The possibility of the presence of well-photosensitized but hypoxic disease in the i.p. cavity requires further investigation, and patients with such disease may perhaps benefit from the augmentation of tumor oxygenation during i.p. PDT. These findings strongly support the addition of methods to measure tumor hypoxia and photosensitizer uptake to future i.p. PDT trials to permit the investigation of a larger patient population and correlation with treatment outcome.

ACKNOWLEDGMENTS

We thank Debbie Smith, RN, and Ruth Collins, RN, for assistance and Deirdre P. Magarelli for technical expertise.

REFERENCES

1. Sadeghi B, Arvieux C, Glehen O, et al. Peritoneal carcinomatosis from non-gynecologic malignancies: results of the EVOCAPE 1 multicentric prospective study. Cancer (Phila) 2000;88:358–63.

2. Miettinen M, Sarlomo-Rikala M, Lasota J. Gastrointestinal stromal tumors: recent advances in understanding of their biology. Hum Pathol 1999;30:1213–20.

3. Cintron JR, Pearl RK. Colorectal cancer and peritoneal carcinomatosis. Semin Surg Oncol 1996;12:267–78.

4. Pilati P, Rossi CR, Mocellin S, et al. Multimodal treatment of peritoneal carcinomatosis and sarcomatosis. Eur J Surg Oncol 2001;27:125–34.

5. Hendren SK, Hahn SM, Spitz FR, et al. Phase II trial of debulking surgery and photodynamic therapy for disseminated intraperitoneal tumors. Ann Surg Oncol 2001;8:65–71.

6. DeLaney TF, Sindelar WF, Tochner Z, et al. Phase I study of debulking surgery and photodynamic therapy for disseminated intraperitoneal tumors. Int J Radiat Oncol Biol Phys 1993;25:445–57.

7. Brown JM, Giaccia AJ. The unique physiology of solid tumors: opportunities (and problems) for cancer therapy. Cancer Res 1998;58:1408–16.

8. Brizel DM, Dodge RK, Clough RW, Dewhirst MW. Oxygenation of head and neck cancer: changes during radiotherapy and impact on treatment outcome. Radiother Oncol 1999;53:113–7.

9. Hockel M, Knoop C, Schlenger K, et al. Intratumoral pO_2 predicts survival in advanced cancer of the uterine cervix. Radiother Oncol 1993;26:45–50.

10. Nordsmark M, Overgaard M, Overgaard J. Pretreatment oxygenation predicts radiation response in advanced squamous cell carcinoma of the head and neck. Radiother Oncol 1996;41:31–9.

11. Sitnik TM, Hampton JA, Henderson BW. Reduction of tumour oxygenation during and after photodynamic therapy in vivo: effects of fluence rate. Br J Cancer 1998;77:1386–94.

12. Foster TH, Hartley DF, Nichols MG, Hilf R. Fluence rate effects in photodynamic therapy of multicell tumor spheroids. Cancer Res 1993;53:1249–54.

13. Henderson BW, Fingar VH. Oxygen limitation of direct tumor cell kill during photodynamic treatment of a murine tumor model. Photochem Photobiol 1989;49:299–304.

14. Henderson BW, Busch TM, Vaughan LA, et al. Photofrin photodynamic therapy can significantly deplete or preserve oxygenation in human basal cell carcinomas during treatment, depending on fluence rate. Cancer Res 2000;60:525–9.

15. Evans SM, Jenkins WT, Joiner B, Lord EM, Koch CJ. 2-Nitroimidazole (EF5) binding predicts radiation resistance in individual 9L s.c. tumors. Cancer Res 1996;56:405–11.

16. Evans SM, Hahn SM, Magarelli DP, et al. Hypoxia in human intraperitoneal and extremity sarcomas. Int J Radiat Oncol Biol Phys 2001;49:587–96.

17. Evans SM, Hahn S, Pook DR, et al. Detection of hypoxia in human squamous cell carcinoma by EF5 binding. Cancer Res 2000;60:2018–24.

18. Ziemer LS, Koch CJ, Maity A, et al. Hypoxia and VEGF mRNA expression in human tumors. Neoplasia 2001;3:500–8.

19. Evans SM, Koch CJ. Prognostic significance of tumor oxygenation in humans. Cancer Lett 2003;195:1–16.

20. Evans SM, Judy KD, Dunphy I, et al. Comparative measurements of hypoxia in human brain tumors using needle electrodes and EF5 binding. Cancer Res 2004;64:1886–92.

21. Laughlin KM, Evans SM, Jenkins WT, et al. Biodistribution of the nitroimidazole EF5 (2-[2-nitro-1*H*-imidazol-1-yl]-*N*-(2,2,3,3,3-pentafluoropropyl) acetamide) in mice bearing subcutaneous EMT6 tumors. J Pharmacol Exp Ther 1996;277:1049–57.

22. Koch CJ, Hahn SM, Rockwell KJ, et al. Pharmacokinetics of the 2-nitroimidazole EF5 [2-(2-nitro-1-*H*-imidazol-1-yl)-*N*-(2,2,3,3,3-pentafluoropropyl)acetamide] in human patients: implications for hypoxia measurements *in vivo*. Cancer Chemother Pharmacol 2001;48:177–87.

23. Bellnier DA, Greco WR, Parsons JC, et al. An assay for the quantitation of Photofrin in tissues and fluids. Photochem Photobiol 1997;66:237–44.

24. Pinheiro J, Bates DM. Mixed-effects models in S and Splus. New York: Springer; 2003.

25. Koch CJ. Measurement of absolute oxygen levels in cells and tissues using oxygen sensors and the 2-nitroimiddazole EF5. In: Sen C, Packer L, editors. Methods in enzymology: antioxidants and redox cycling, vol. 352. San Diego, CA: Academic Press, 2002. p. 3–31.

26. Lartigau E, Lusinchi A, Eschwege F, Guichard M. Tumor oxygenation: the Institut Gustave Roussy experience. In: Vaupel P, Kelleher DK, editors. Tumor hypoxia pathophysiology, clinical significance and therapeutic perspectives. Stuttgart, Germany: Wissenschaftliche Verlagsgesellschaft mbH; 1999. p. 47–52.

27. Vaupel P, Hockel M. Oxygenation status of breast cancer: the Mainz experience. In: Vaupel P, Kelleher DK, editors. Tumor hypoxia pathophysiology, clinical significance and therapeutic perspectives, Stuttgart, Germany: Wissenschaftliche Verlagsgesellschaft mbH; 1999. p. 1–11.

28. Nordsmark M, Overgaard J. Oxygenation of human tumors: the Aarhus experience. In: Vaupel P, Kelleher DK, editors. Tumor hypoxia pathophysiology, clinical significance and therapeutic perspectives Stuttgart, Germany: Wissenschaftliche Verlagsgesellschaft mbH; 1999. p. 19–27.

29. Menon C, Kutney SN, Lehr SC, et al. Vascularity and uptake of photosensitizer in small human tumor nodules: implications for intraperitoneal photodynamic therapy. Clin Cancer Res 2001;7:3904–11.

30. Busch TM, Wileyto EP, Emanuele MJ, et al. Photodynamic therapy creates fluence rate-dependent gradients in the intratumoral spatial distribution of oxygen. Cancer Res 2002;62:7273–9.

31. Khan S, Cleveland RP, Koch CJ, Schelling JR. Hypoxia induces renal tubular epithelial cell apoptosis in chronic renal disease. Lab Investig 1999;79:1089–99.

32. Bergeron M, Evans SM, Sharp FR, et al. Detection of hypoxic cells with the 2-nitroimidazole, EF5, correlates with early redox changes in rat brain after perinatal hypoxia-ischemia. Neuroscience 1999;89:1357–66.

33. Evans SM, Laughlin KM, Pugh CR, Sehgal CM, Saunders HM. Use of power Doppler ultrasound-guided biopsies to locate regions of tumour hypoxia. Br J Cancer 1997;76:1308–14.

34. Bialik S, Geenen DL, Sasson IE, et al. Myocyte apoptosis during acute myocardial infarction in the mouse localizes to hypoxic regions but occurs independently of p53. J Clin Investig 1997;100:1363–72.

35. Clyman RI, Chan CY, Mauray F, et al. Permanent anatomic closure of the ductus arteriosus in newborn baboons: the roles of postnatal construction, hypoxia, and gestation. Pediatr Res 1999;45:19–29.